

See discussions, stats, and author profiles for this publication at: <https://www.researchgate.net/publication/262264870>

Drying and denaturation characteristics of α -LACTALBUMIN, β -lactoglobulin, and bovine serum albumin in a convective drying process

ARTICLE in JOURNAL OF AGRICULTURAL AND FOOD CHEMISTRY · MAY 2014

Impact Factor: 2.91 · DOI: 10.1021/jf405603c · Source: PubMed

CITATIONS

8

READS

89

5 AUTHORS, INCLUDING:



Md. Amdadul Haque

RMIT University Melbourne Australia

11 PUBLICATIONS 39 CITATIONS

[SEE PROFILE](#)



Peter Aldred

Federation University Australia

52 PUBLICATIONS 1,152 CITATIONS

[SEE PROFILE](#)



Jie Chen

Second Military Medical University, Shanghai

282 PUBLICATIONS 2,789 CITATIONS

[SEE PROFILE](#)



Benu Adhikari

RMIT University

185 PUBLICATIONS 1,894 CITATIONS

[SEE PROFILE](#)

Drying and Denaturation Characteristics of α -Lactalbumin, β -Lactoglobulin, and Bovine Serum Albumin in a Convective Drying Process

M. Amdadul Haque,^{†,‡} Peter Aldred,[§] Jie Chen,[#] Colin Barrow,[⊥] and Benu Adhikari^{*,†}

[†]School of Applied Sciences, RMIT University, Melbourne City Campus, Melbourne, VIC 3001, Australia

[‡]Department of Agro-processing, BSMRAU, Gazipur 1706, Bangladesh

[§]School of Health Sciences, University of Ballarat, Mount Helen, VIC 3353, Australia

[#]State Key Laboratory for Food Science and Technology, Jiangnan University, Wuxi, China

[⊥]School of Life and Environmental Sciences, Deakin University, Geelong, VIC 3217, Australia

ABSTRACT: Drying and denaturation kinetics of aqueous droplets of α -lactalbumin (α -lac), β -lactoglobulin (β -lg), and bovine serum albumin (BSA) were measured in a convective drying environment. Single droplets having an initial droplet diameter of 2 ± 0.1 mm and containing 10% (w/v) protein concentration were dried using conditioned air (65 and 80 °C, 2–3% RH, 0.5 m/s velocity) for 600 s. The denaturation of these proteins was measured by using reversed-phase HPLC. At the end of 600 s of drying 13.3 and 19.4% α -lac was found to be lost due to denaturation at 65 and 80 °C, respectively. Up to 31.0% of β -lg was found to be denatured, whereas BSA was not found to be significantly ($p > 0.05$) denatured in these drying conditions. The formation and strength of skin and the associated morphological features were found to be linked with the degree of denaturation of these proteins. The secondary structure of these proteins was significantly ($p < 0.05$) affected and altered by the drying stresses. The β -sheet and random coil contents were increased in α -lac by 6.5 and 4.0%, respectively, whereas the α -helix and β -turn contents decreased by 5.5 and 5.0%, respectively. The β -sheet and random coil contents in β -lg were increased by 7.5 and 2.0%, respectively, whereas the α -helix and β -turn contents decreased by 3.5 and 6.0%, respectively. In the case of BSA the β -sheet, α -helix, and random coil contents were found to increase, whereas the β -turn content decreased.

KEYWORDS: bovine serum albumin, α -lactalbumin and β -lactoglobulin denaturation, drying, single droplet, β -sheet, β -turn, α -helix, morphology

INTRODUCTION

Whey is a heterogeneous mix of proteins. Among these proteins, α -lactalbumin (α -lac, 20%), β -lactoglobulin (β -lg, 65%), and bovine serum albumin (BSA, 8%) are the major constituents and comprise >90% of total whey protein. There are numerous studies in the literature reporting the denaturation of whey protein during thermal processing including drying.^{1–3} However, these studies do not provide the drying and denaturation kinetics of individual whey protein fractions. A limited number of works are reported in the literature that provide the extent of denaturation of individual whey proteins (when they are treated separately), especially during isothermal heat treatment and high-pressure treatment processes.^{4–6} There is little, if any, published work in the literature quantifying and analyzing the denaturation kinetics of individual whey protein components at the droplet level during convective drying. The quantification and understanding of drying and denaturation kinetics of individual whey protein components can help minimize the denaturation of individual whey proteins during powder formation and also help in designing better spray-dryers.

The spray-drying process involves atomization of a solution into droplets in a drying chamber and subsequent removal of the solvent through evaporation and finally formation of powder product. The formation of particles from a solution in the convective drying process such as spray-drying involves

both equilibrium thermodynamic and kinetic processes. The vapor pressure and temperature gradients within a drying droplet and the drying medium are the key driving forces for the mass transfer from, and heat transfer to, the droplet. In an actual drying process, unique and complex evolution of particle shape and morphology takes place, which affects the mass and heat transport process. On the other hand, the magnitude of the vapor pressure and temperature gradients and the resultant heat and mass transfer fluxes also greatly affect the development of morphology in drying droplets.

In the spray-drying process, the operating parameters (or even the design of dryer to less extent) have to be judiciously selected to control the particle morphology. This is because the characteristics of the product such as particle density, particle size distribution, and residual final moisture content are greatly affected by the morphology of dried particles.⁷ During spray-drying, the particle morphology is greatly affected by the drying conditions as well as by the nature and concentration of feed and the mode of atomization used. For example, the skin-forming and crust-forming materials develop quite different

Received: January 5, 2014

Revised: May 1, 2014

Accepted: May 1, 2014

Published: May 2, 2014



morphological features.⁸ Hence, the monitoring and analysis of the evolution of morphology during the particle formation process can provide very important information. However, it is not yet technologically feasible to capture the evolution of morphology during the particle formation process *in situ* during spray-drying. To date, the morphological features of spray-dried powders are acquired and analyzed using final powder particles.⁹ However, these morphological features cannot be used to explain the evolution of morphology during the particle formation process. Thus, the relationships among the drying kinetics, morphology, physicochemical characteristics, and denaturation of protein are poorly understood. Single-droplet drying experiments are commonly carried out to capture the evolution of morphological features in drying droplets in convective drying processes.¹⁰ Despite some limitations such as much larger droplet size and much longer drying time, single droplet drying experiments provide very important information regarding the development of morphological features during the convective drying process which is a much simplified and idealized model of spray-drying.^{11–14}

Reversed-phase high-performance liquid chromatography (RP-HPLC) is an effective tool to separate denatured and native proteins. The chemical resin in the stationary phase of this column (i.e., presence of C8, C18) successfully retards migration of the denatured protein.^{3,15} The strong affinity of these chemicals toward the hydrophobic portion of denatured proteins helps to separate the denatured and native proteins.

The functionality of protein predominantly depends on its specific molecular composition and structure. The polypeptide chains acquire a folded form to perform their biological functions. However, the stress generated during processing such as spray-drying can alter the structure of protein. Fourier transform infrared (FTIR) spectroscopy has been commonly used to identify and explain the structural characteristics of proteins. It is used to quantify the change in the secondary structure of proteins.¹⁶ The polypeptide and protein repeat units give rise to nine characteristic IR absorption bands, namely, amides A and B and amides I–VII. The amide I region ranging between 1600 and 1700 cm⁻¹ is commonly chosen to measure qualitative and quantitative changes in secondary structure of proteins because of its very high signal-to-noise ratio.^{17,18} Furthermore, the absorption at this band is able to give considerable variation in IR signal even at small alterations in the molecular configuration of analytes.¹⁹

Although the IR spectra obtained are intrinsic and complex, mathematical tools such as derivatization and Fourier self-deconvolution (FSD) analyses are available to determine the unique structural features such as α -helix, β -sheets, β -turns, and random coils of a protein.^{20,21} The derivatization and FSD can be applied to quantify alteration in structural features of proteins due to processing stresses.^{16,17}

In this context, the key aim of this study was to measure the denaturation and drying kinetics of major whey proteins (α -lac, β -lg, and BSA) in convective air-drying environments. FTIR spectroscopy was used to quantify and explain the alteration in the secondary structure of these proteins caused by drying-induced stresses. The evolution of droplet morphology was captured and analyzed using single-droplet drying experiments.

EXPERIMENTAL PROCEDURES

Materials. The protein samples (α -lac, β -lg, and BSA) with high purity ($\geq 95\%$ pure) were purchased from Sigma-Aldrich (New South Wales, Australia). The HPLC solvents acetonitrile and trifluoroacetic

acid (TFA) were purchased from Sigma-Aldrich and Fisher Scientific (Victoria, Australia), respectively. Deuterium oxide (D_2O) was purchased from Sigma-Aldrich. All proteins and chemicals were used as received without further purification.

Methods. *Single-Droplet Drying (SDD).* Details of the SDD instrument and its working procedure are provided elsewhere.^{22,23} Aqueous droplets of $5 \pm 0.1 \mu L$ initial volume (2 ± 0.1 mm initial droplet diameter) containing 10% (w/v) protein were suspended on the tip of a glass filament with a 0.2 ± 0.01 mm diameter. This droplet-suspending filament was supported by a droplet suspension system made up of a bored Teflon cylinder. The droplets were then subjected to conditioned drying air. The drying air was cleaned and heated by passing through a series of columns containing dried molecular sieve and dried silica gel. The temperature of the drying air was controlled by a proportional-integral-derivative (PID) controller. The droplets were dried at two different air temperatures (65 and 80 °C) at a constant velocity of 0.5 m/s. The relative humidity of the drying air was measured by using an EL-USB relative humidity data logger (Lascar Electronics, UK) and was found to be $2.5 \pm 0.5\%$ at these two drying temperatures. The wet bulb temperatures corresponding to air temperatures of 65 and 80 °C were 26 and 30 °C, respectively. The droplets were dried for 600 s, and the denaturation was measured at every 60 s interval. The temperature and mass loss histories were recorded in a computer. Images of the droplets during drying were captured at every 50 s interval using a digital camera (EOS 60D, Canon, NSW, Australia) at 40–50× magnification.

Determination of Denaturation of Proteins. The convectively dried droplets were diluted to 100 µg/mL with deionized water. Then, the pH of the diluted protein solutions was lowered to 4.6 by adding 0.1 M HCl to assist in separating the native and denatured proteins.^{23,24} After the pH of protein solutions was adjusted, they were kept for 30 min and centrifuged at 11500g for 10 min. The supernatant was collected and injected onto the RP-HPLC column to separate the denatured and undenatured proteins. A control sample without drying was treated in the same way including pH treatment and centrifugation. The supernatant of the control sample was also subjected to RP-HPLC separation in the same way as dried protein. Residual native protein content was calculated using the ratio between the area under the peak of the treated protein and the area under the peak of untreated (control) protein (100%), as suggested by Parris and Baginski.³

The experiments were carried out in triplicate, and the average values are reported in the ensuing sections. The statistical analyses were carried out by using data analysis tools, Microsoft Office Excel 2010. The significance difference between two mean values was determined using one-way analysis of variance at 95% confidence level ($p < 0.05$). The inbuilt program in Microsoft Excel was used for this purpose.

Acquiring the IR Spectra. The IR spectra were acquired using a PerkinElmer Frontier FT-IR instrument operated by CPU32 M software. The SDD samples subjected to single-droplet drying and control samples were diluted to 5 mg/mL concentration using deuterium oxide (D_2O) containing 100 mM sodium chloride (NaCl).¹⁸ The samples used in these tests were collected after 500 s of drying at both drying (air) temperatures. This time of sample collection (500 s) was chosen on the basis of the fact that both WPI (as a whole) and its major component β -lg were found to reach their maximum levels of denaturation at this time at both drying temperatures.²⁵ The samples were scanned within 650–4000 cm⁻¹ using triglycine sulfate (TGS) detector. A total of four scans at 4 cm⁻¹ resolution were accumulated at 0.2 cm/s scanning speed.

Analysis of IR Spectra. The blank spectrum ($D_2O + NaCl$) was subtracted from the spectrum of each sample. The baseline-subtracted protein spectra were analyzed by using PerkinElmer's proprietary software (version 10.03.06) and OPUS 6.5.92 (Bruker Biosciences Pty Ltd., Victoria, Australia). A 9-point second-derivative analysis using the PerkinElmer software was used to locate the peak position in the spectra. The OPUS software was used for quantitative analysis of secondary structure of protein by Fourier self-deconvolution. The original spectra (of amide region I, 1600–1700 cm⁻¹) without any

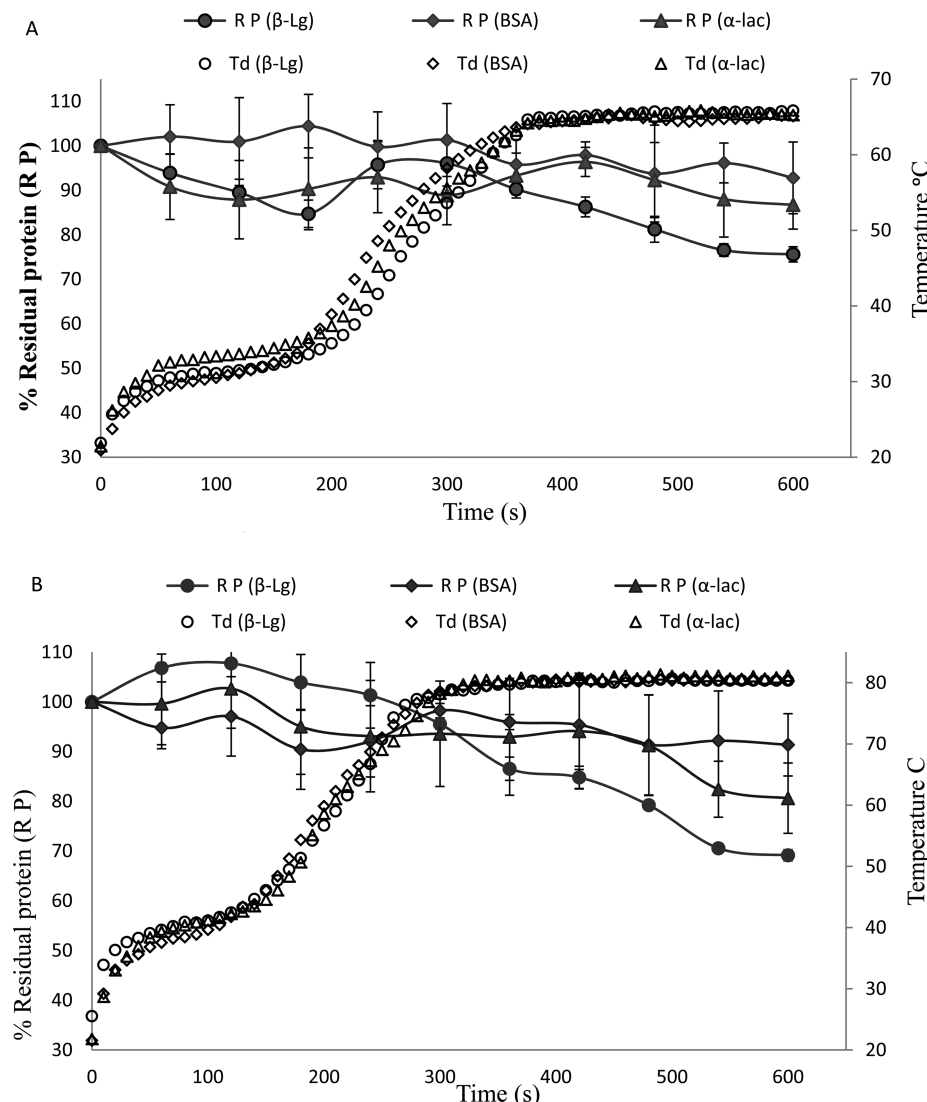


Figure 1. Denaturation of BSA, α -lac, and β -lg with drop temperature increment during drying at (A) 65 and (B) 80 $^{\circ}$ C air temperatures. The error bars show the standard deviation (SD) of experimental values.

smoothing were deconvoluted by gamma factor 2. The FSD curves were fitted with Gaussian shape and were analyzed by local least-squares (LLS) algorithm. Percentage of secondary structures (α -helix, β -sheets, β -turns, and random coils) was estimated using eq 1^{16,26}

$$\text{secondary structure (\%)} = A_{\text{ind}} / A_{\text{total}} \times 100 \quad (1)$$

where A_{ind} = sum of area of individual secondary structure in amide I band and A_{total} = sum of area of total secondary structure in amide I band.

The position or location of bands for each secondary structure (β -sheets, α -helix, and β -turns) of tested proteins in D_2O were determined as suggested in the literature.^{19,27,28} The bands from 1620 to 1640 cm^{-1} and from 1674 to 1680 cm^{-1} were assigned to β -sheets. The bands from 1641 to 1647 cm^{-1} were assigned to random coil. The bands within 1648–1660 cm^{-1} were assigned to α -helix. Similarly, the bands appearing at and in the vicinity of 1663, 1671, 1683, 1688, and 1694 cm^{-1} were assigned to β -turns.

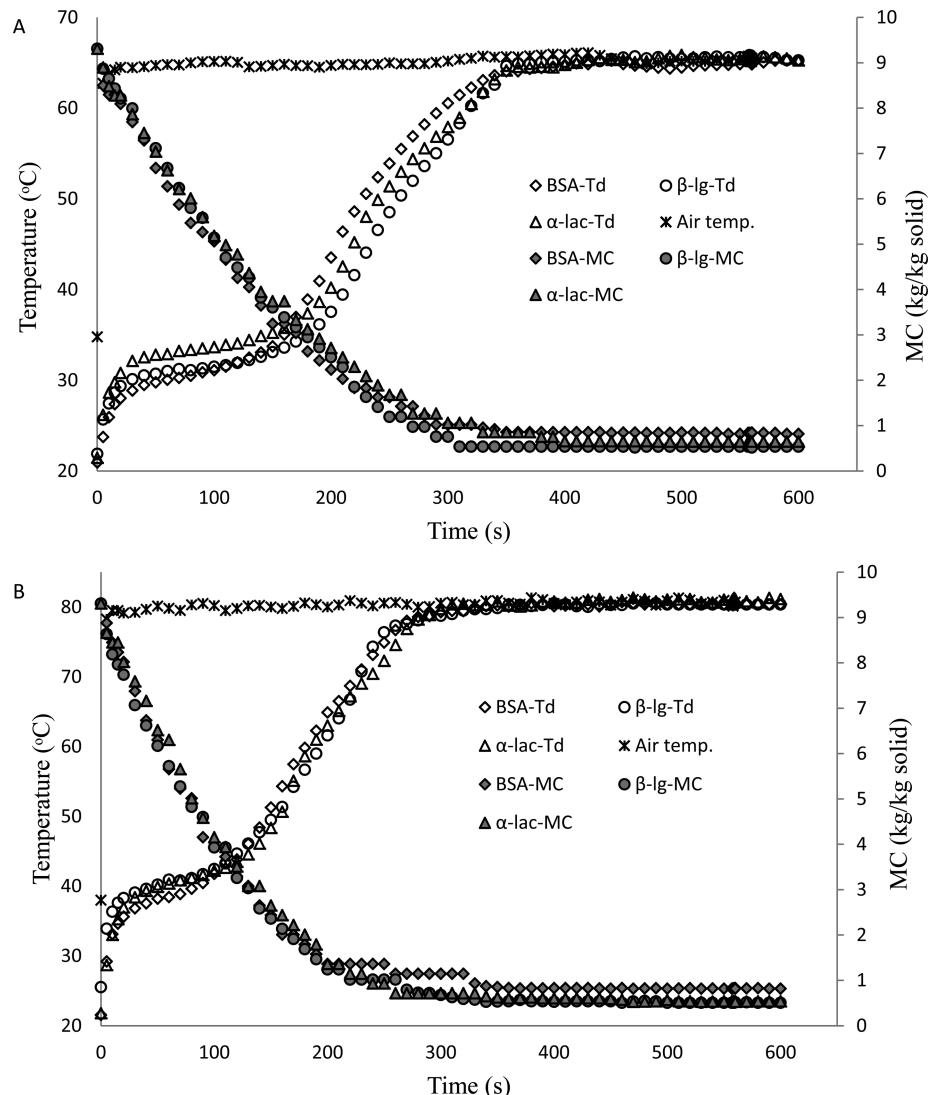
RESULTS AND DISCUSSION

Denaturation of BSA, β -Lg, and α -Lac during Convective Drying. The denaturation kinetics of BSA, β -lg, and α -lac due to convective drying at droplet level were measured by RP-HPLC. As presented in Figure 1, a different

extent of denaturation was observed in these whey protein fractions. Among these three proteins, BSA showed the highest stability as determined by the highest level of residual protein. β -Lg showed the least stability, that is, the lowest level of residual protein during drying. The stability of α -lac against denaturation remained between those of BSA and β -lg at both 65 and 80 $^{\circ}$ C (Figure 1). There was no significant ($p > 0.05$) loss of BSA and α -lac when dried at 65 and 80 $^{\circ}$ C for up to 480 s. At the end of 600 s, 13.26 and 19.37% of α -lac was found to be denatured at 65 and 80 $^{\circ}$ C, respectively. When the solution of β -lg was dried at these two drying temperatures, 24.40 and 30.85% of this protein was found to be denatured at 65 and 80 $^{\circ}$ C drying temperatures, respectively, when dried for 600 s. The difference in molecular configuration of these protein fractions might have played an important role for these differences in the observed denaturation. Specifically, the difference in the number of cysteine (amino acid) molecules and sulfur bridges in the structure of these proteins can be attributed to the variation in the denaturation. β -Lg starts to show significant ($p < 0.05$) loss due to denaturation (Figure 1B) when it reaches a state of irreversible denaturation (for example, 240 s at 80 $^{\circ}$ C). Before this state of irreversible denaturation is reached,

Table 1. Model Constants To Predict the Evaporation Rate from Droplets during Drying of α -Lac, β -Lg, and BSA

drying temp (°C)	protein	model constants				R^2
		A	B	C	D	
65	α -lac	$6.65e^{-6}$	0.00507	0.9740		0.98 ± 0.02
	β -lg	$7.5e^{-6}$	0.0055	0.9940		
	BSA	$8.6e^{-6}$	0.0058	0.9770		
80	α -lac	$1.3e^{-8}$	$1.75e^{-5}$	0.0074	0.9968	0.97 ± 0.03
	β -lg	$1.6e^{-8}$	$2.00e^{-5}$	0.0078	0.9728	
	BSA	$1.6e^{08}$	$2.00e^{-5}$	0.0078	0.9728	

Figure 2. Moisture content and temperature profiles of BSA, α -lac, and β -lg during drying at (A) 65 and (B) 80 °C drying temperature. MC, moisture content; Td, drop temperature.

reversible denaturation occurs, and it involves excitation (due to the affinity of reaction of the thiol group of free cysteine with the adjacent sulfur bonds) of free cysteine molecules present in the β -lg and BSA structures. Due to prolonged drying stress, the peptides of β -lg are exposed to such an extent that they start to aggregate. On the other hand, the presence of 17 sulfur bridges helps to keep BSA relatively stable. Due to the absence of any free cysteine in α -lac structure, this protein is comparatively less excited or perturbed when it is subjected to dehydration stresses and it is less affected by thiol–disulfide

interaction.²⁹ A more detailed explanation of the factors causing different extents of denaturation of these whey protein constituents during convective drying is presented elsewhere.²⁵

Drying Kinetics and Its Relationship with Protein Denaturation. It is shown in Figure 1 that all of the denaturation–time curves exhibit some degree of fluctuation or perturbation from the very beginning of the drying process. When the droplet temperature was about 40 ± 5 °C, the denaturation–time curves started to fluctuate due to the impact of drying on the surface hydrophobicity. β -lg started to be lost

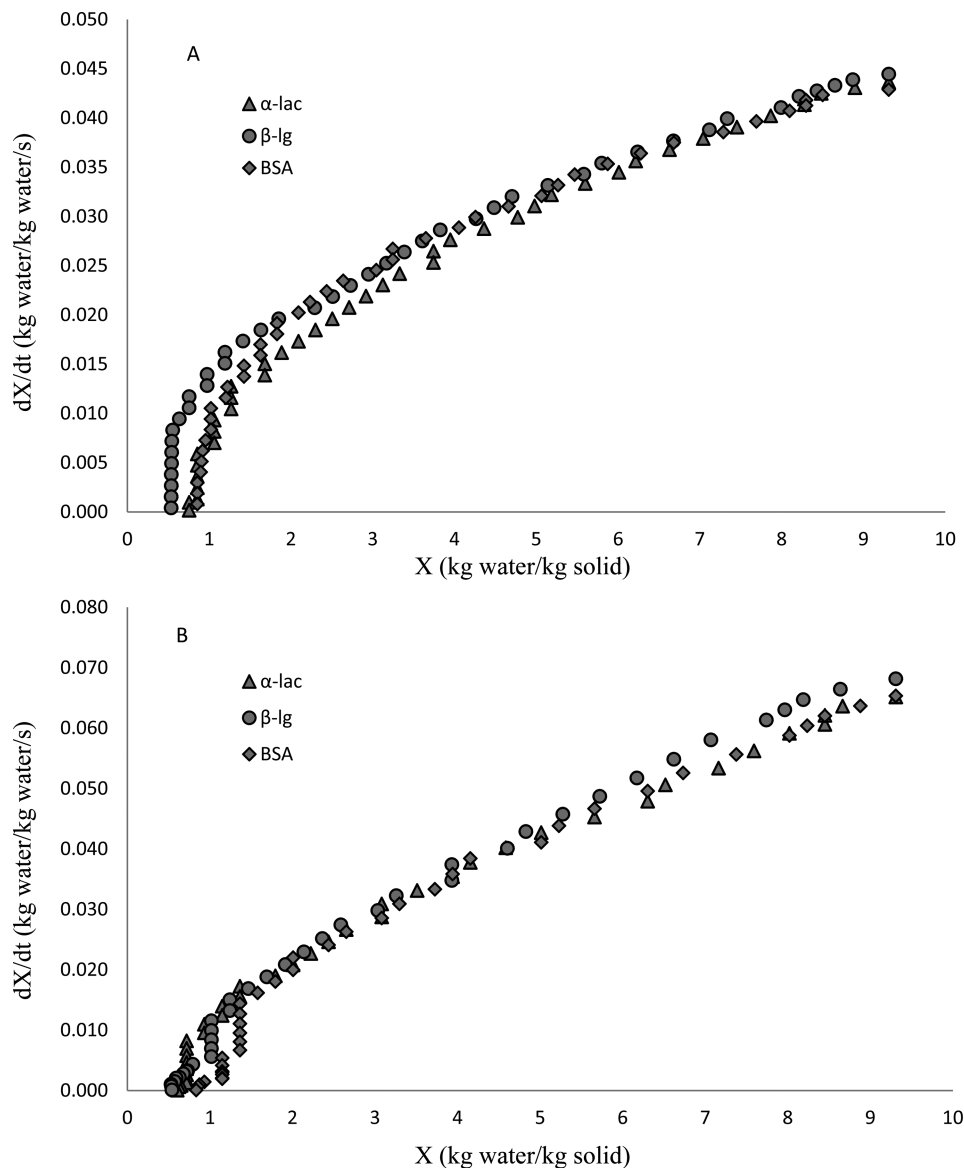


Figure 3. Evaporation rate profiles as a function of water content during drying of α -lac, β -lg, and BSA droplets at (A) 65 and (B) 80 °C air temperature.

due to irreversible denaturation and subsequent coagulation when the droplet temperature reached 55 ± 5 °C (Figure 1A). This irreversible denaturation started becoming prominent at 290 and 240 s of drying at 65 and 80 °C, respectively. We had previously reported the relationship between denaturation and droplet temperature in the case of WPI.²⁵ A similar trend in the relationship between denaturation and drying temperature was observed in this study only in the case of β -lg. The trends in the relationship between drying temperature and denaturation in the case of BSA and α -lac are quite different. In our earlier study,²⁵ WPI was dried and the individual fractions of WPI (α -lac, β -lg, and BSA) were dried as a part of whole. In the current study, intact and native individual proteins (α -lac, β -lg, and BSA) were dried individually as starting materials and the denaturation kinetics of one is not affected by the presence of the others.

To better understand the effect of drying rate on the protein denaturation, we determined the drying rate (dX_t/dt) from the experimental moisture loss versus time data. Polynomial models

were fitted with the experimental moisture ratio (MR), and the drying rate was determined as shown by eqs 3 and 5 below.

For 65 °C drying temperature:

$$MR = \frac{X_t - X_\infty}{X_0 - X_\infty} = At^2 - Bt + C \quad (2)$$

$$\frac{dX_t}{dt} = (X_0 - X_\infty)(2At - B) \quad (3)$$

For 80 °C drying temperature:

$$MR = \frac{X_t - X_\infty}{X_0 - X_\infty} = -At^3 + Bt^2 - Ct + D \quad (4)$$

$$\frac{dX_t}{dt} = (X_0 - X_\infty)(-3At^2 + 2Bt - C) \quad (5)$$

X_t = moisture content of the droplet being dried at a given time (kg/kg solid), X_∞ = final moisture content of the dried droplet at the end of drying (kg/kg solid), and X_0 = initial moisture

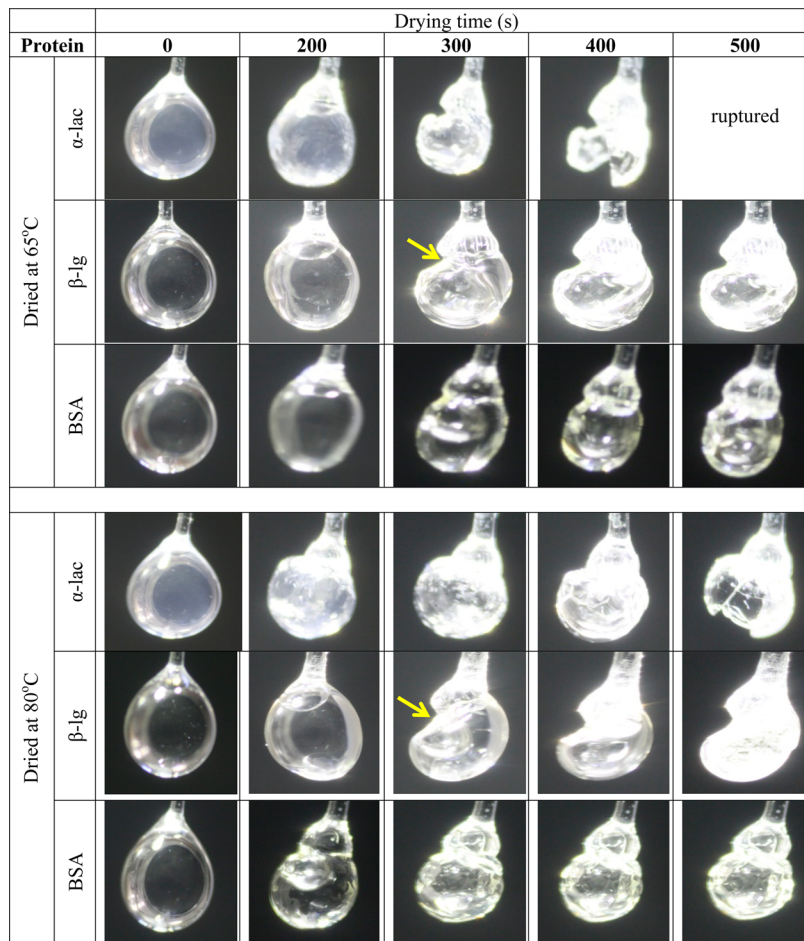


Figure 4. Development of morphological features in α -lac, β -lg, and BSA during single droplet drying at 65 and 80 °C. The arrows show partial loss of spherical shape.

content of the droplet being dried (kg/kg solid). Similarly, t = drying time (s), and A , B , C and D are the model constants. After fitting the moisture ratio curves with acceptable R^2 values, the drying rates (dX_t/dt) for all of the protein samples were calculated as shown by eqs 3 and 5. The estimated model constants along with the R^2 values are listed in Table 1.

The drying kinetics (moisture content and temperature histories) of BSA, β -lg, and α -lac are presented in Figures 2 and 3. It can be seen from Figures 2A and 3A that the BSA and β -lg tended to show higher rate of moisture loss (0.0218 and 0.0213 kg water/kg dry solid/s, respectively) than α -lac (0.0200 kg water/kg dry solid/s), and their droplet temperature remained close to the wet bulb temperature up to around 200 s. It also appears that an increase in BSA concentration offers greater resistance to moisture removal. The difference in the drying kinetics between these two proteins is observed after 200 s, and the drying rate of BSA became lower than that of β -lg (Figure 3A). After about 390 s of drying at 65 °C, the moisture content of both proteins did not decrease further and the droplet temperatures also reached very close to the drying air temperature. After the transition period of 200 s, the trends in the droplet temperature histories of these two proteins also changed remarkably. The temperature of the BSA droplet increased more rapidly than that of β -lg. In the case of α -lac the drop temperature started to increase more quickly than those of BSA and β -lg. The α -lac also showed similar reversible–irreversible transition at 200 s while drying at 65 °C. After this

point, the droplet temperature of α -lac increased very rapidly and reached close to the drying air temperature. The rate of increase in droplet temperature in α -lac was faster than that of β -lg but slower than that of BSA.

These transitions in the temperature history curves (Figure 2A) of these proteins stem from the increased “drop side resistance” to the outward diffusion of moisture content.⁸ The increased resistance to outward moisture diffusion gives rise to the “profile reversal”, which means that the droplet temperature of the usually slower drying droplet is higher. Before the profile reversal, the drop temperature of β -lg droplet is slightly higher than that of BSA. After the profile reversal, the temperature of the BSA droplet is higher than that of the β -lg droplet. This phenomenon is more prominent in the cases of α -lac and BSA. The morphological changes of these protein droplets during convective drying, to some extent, might also be responsible for these interesting features observed in the drying profiles.

The morphological features of droplets of BSA, β -lg, and α -lac while drying at 65 and 80 °C are presented in Figure 4. It can be seen from this figure that the original spherical shape of the droplet remained more or less intact up to 200 s in all of the protein droplets. It has to be pointed out here that so long as the moisture content of the droplet is high and the droplet temperature is not too close to the drying air temperature (Figures 2 and 3), the morphology of the droplet remains more or less spherical (Figure 4). The morphology of these protein droplets showed different trends after 200 s. The BSA was

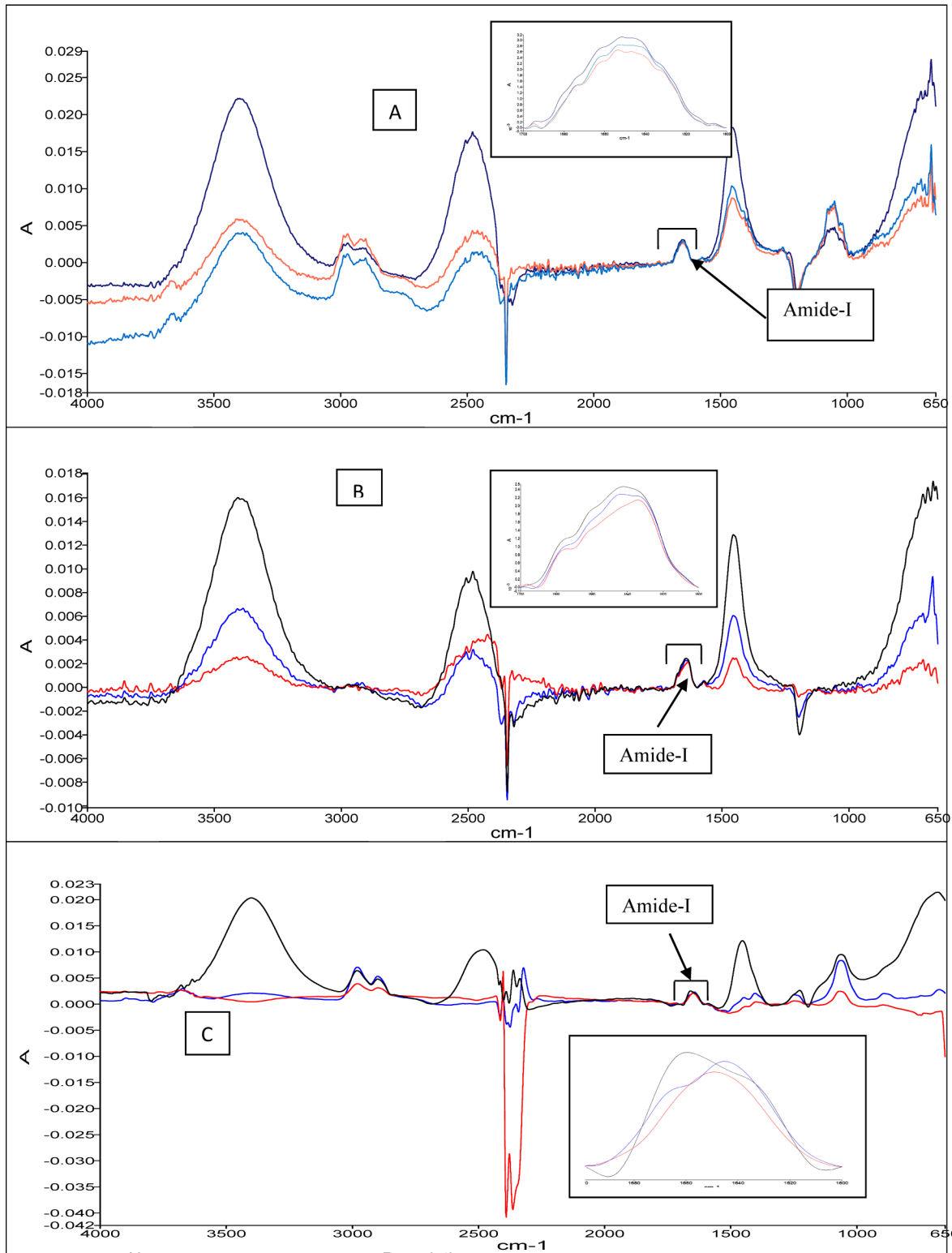


Figure 5. Absorbance spectra from FTIR of original and dried (A) α -lac, (B) β -lg, and (C) BSA (black, blue, and red lines indicate native and 65 and 80 °C treated spectra, respectively). Amide I regions are zoomed in the insets.

capable of retaining more moisture in its matrix and exhibited a sharper increase in droplet temperature. It is commonly accepted that a droplet with a lower drying rate (retains more moisture content) shows faster increase in droplet temperature due to a lesser degree of evaporative cooling. One of the interesting features associated with the morphology and

drying kinetics was that the protein (BSA) containing more water in droplet for longer time was found to retain its spherical shape longer. In addition, the entrapped water inside the drying droplet of this protein caused a buildup of vapor pressure, which developed wrinkles and troughs or uneven surface morphology.³⁰ The interplay between the force generated by

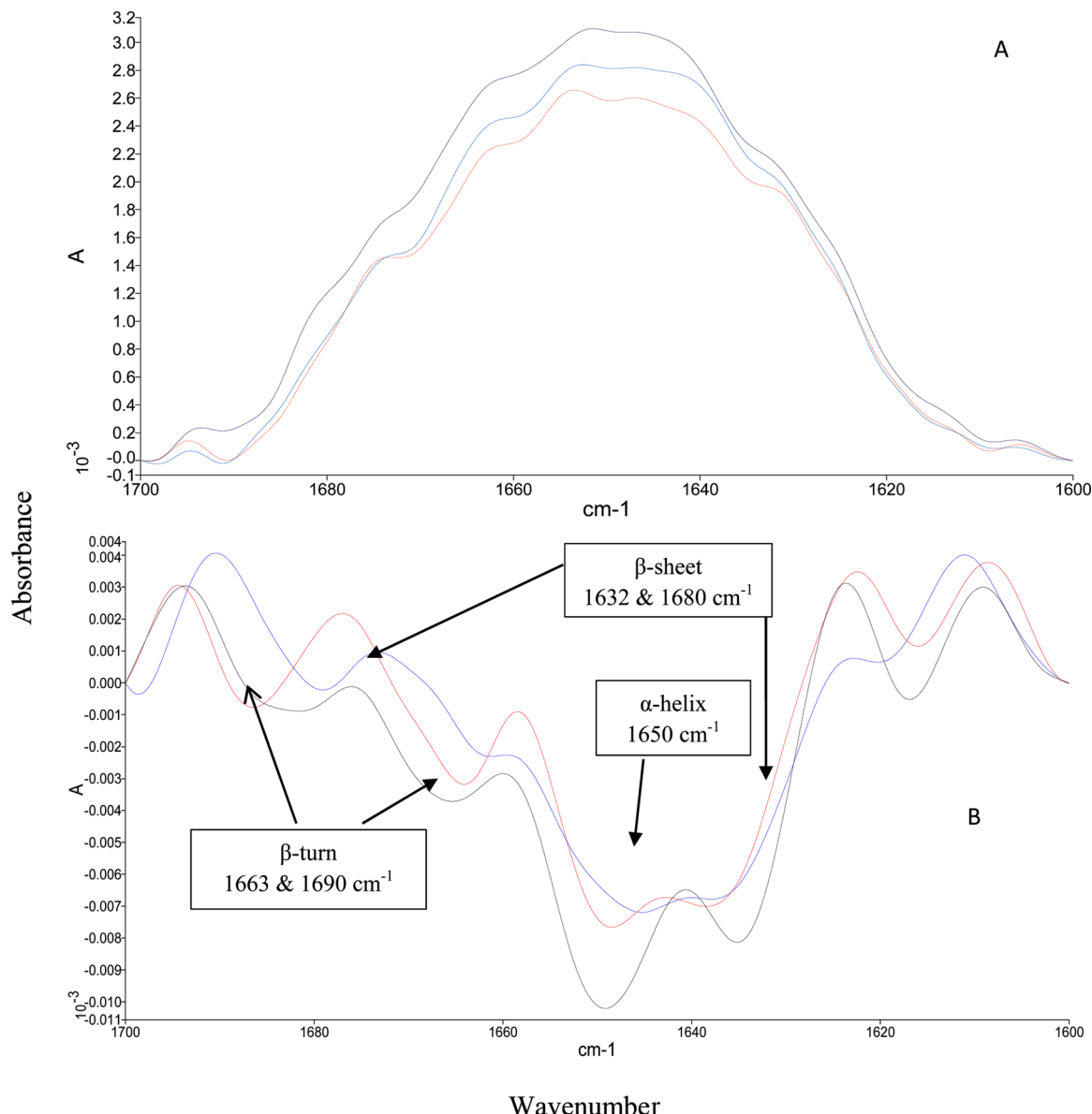


Figure 6. (A) Absorbance and (B) second-derivative spectra of amide I region of the native and single droplet dried α -lac (black, blue, and red lines indicate native and 65 and 80 °C treated spectra, respectively).

this vapor built up within the droplet, and the thermoplastic nature of the protein skin is the one of the main causes giving rise to the wrinkled morphology in BSA. A similar trend regarding the relationship between the surface morphology and drying kinetics was observed in these proteins at 80 °C as well. The only difference was that the development of morphological features occurred much more rapidly while drying at 80 °C. After 360 s of drying at 80 °C, the moisture loss of all three proteins was almost ceased.

Denaturation of BSA, α -Lac, and β -Lg and Droplet Morphology. The evolution of morphology in BSA, α -lac, and β -lg droplets when dried at 65 and 80 °C is presented in Figure 4. As can be seen from this figure, these three proteins produced three different types of morphological features. The surface of the BSA droplet showed the ability to resist the stress exerted by the drying process and, hence, maintained spherical feature and resisted surface folding and wrinkling to a greater extent at both temperatures until the end of drying. β -Lg was least capable of resisting the deformation of droplet/particle

surface during drying at both temperatures. β -Lg partially lost its spherical shape after 300 and 200 s when dried at 65 and 80 °C, respectively, and resulted in a buckled particle. α -Lac maintained its spherical shape during the early stage of drying. However, it started becoming increasingly fragile, and the particle surface was ruptured when the drying progressed.

The whey protein BSA acquired a rigid structure immediately after the start of drying (Figure 4), which might be responsible for much slower moisture evaporation in this protein. The rigidity of the BSA droplet surface during drying might be explained by its large molecular mass. BSA has a higher molecular mass (66.27 kDa) than those of α -lac (14.18 kDa) and β -lg monomer (18.28 kDa). Besides, the high number of sulfur bridges present in the BSA structure might provide greater resistance against outward moisture diffusion and maintain a moist interior. The preservation of its spherical shape by α -lac in the early stage of drying can also be attributed to its skin-forming behavior. The subsequent rupture of the α -lac particle suggests that this protein forms a thinner skin. The

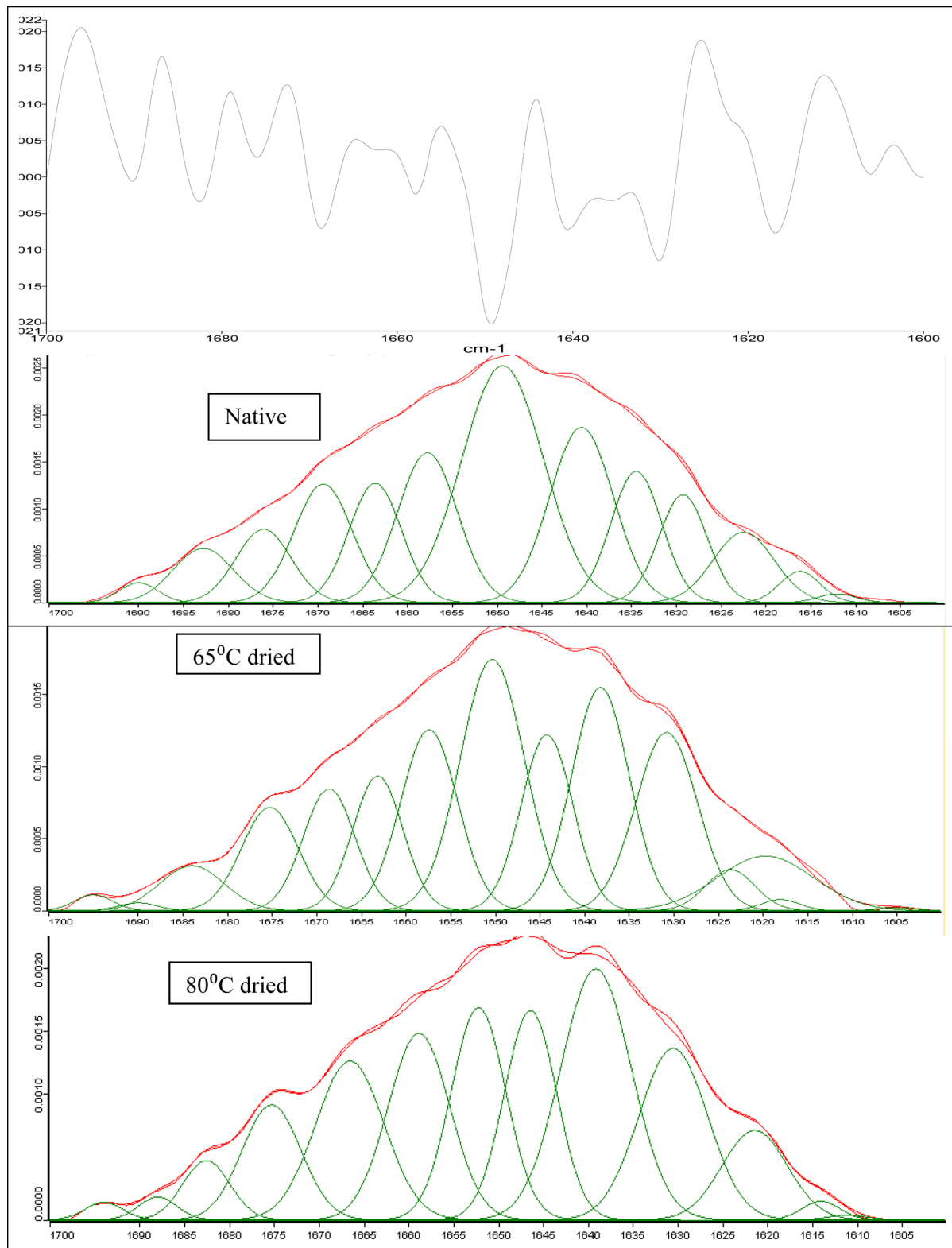


Figure 7. Fitted spectra of native and dried α -lac (a sample of second-derivative spectra of native α -lac is at the top).

irreversible denaturation of proteins and their agglomerates is capable of forming a thick skin at the outer surface of droplets being dried.⁹ It can be observed from Figure 1 that α -lac denatured only marginally at 500 s when the skin was ruptured due to drying (a 65 °C). This lack of denaturation and, hence, the lack of formation of a rigid wall (or skin) produced α -lac particles with a hollow crust. The dried particles with a hollow

crust are known to collapse or shrivel quite easily.⁹ This is why the particles of α -lac ruptured quite easily at both drying temperatures. On the other hand, β -Ig experienced significant ($p < 0.05$) denaturation at both drying temperatures and the denaturation and aggregation occurred as early as 250 s of drying. Because the denatured proteins conveniently form a rigid skin, the formation of skin in this protein also started after

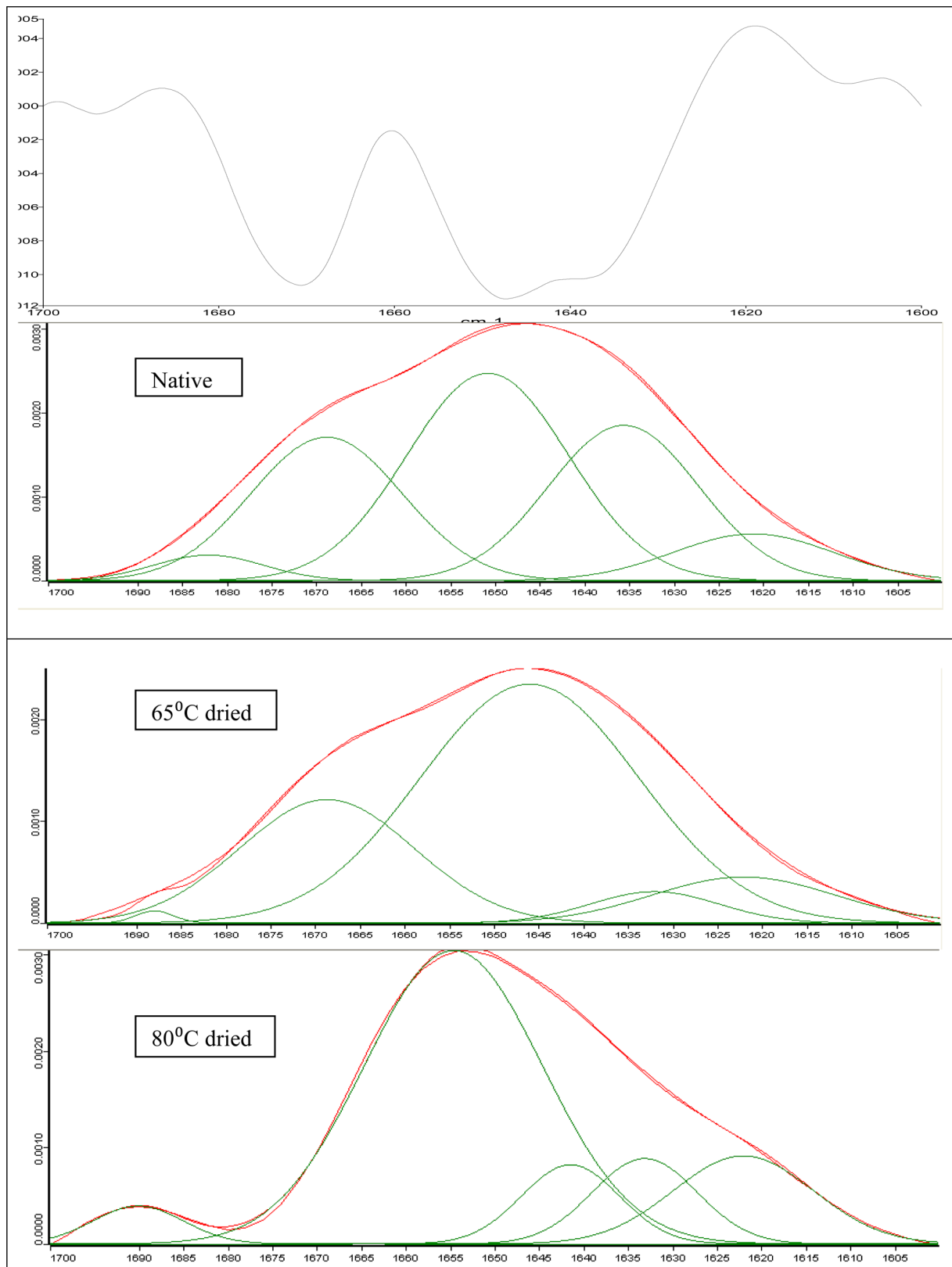


Figure 8. Fitted spectra of native and dried BSA (a sample of second-derivative spectra of native BSA is at the top).

200 s. This explains why the partial wrinkling appeared on the surface of this protein after 200 s. The better stability of α -lac droplet/particle (lack of rupture) at 80 °C compared to 65 °C (Figure 4, 500 s) can be attributed to the significantly ($p <$

0.05) higher extent of denaturation of α -lac at 80 °C than at 65 °C.

Alteration in Secondary Structure of BSA, α -Lac, and β -Lg. Figure 5 shows the IR spectra of native and dried BSA, α -lac, and β -lg. The second derivatives of the IR spectra were

used to identify the individual structural features of these proteins. For example, the derivative spectra (Figure 6B) derived from intrinsic absorbance spectra (Figure 6A) are able to clearly assign some specific bands in both native and dried proteins. The derivative spectra are also able to quantify the magnitude and direction of change occurring in a specific band due to drying-related stresses. For example, when α -lac was dried at 65 °C for 500 s (Figure 6B), the proportion of its β -sheet increased (around 1680 cm⁻¹), and this increase was compensated by the decrease in α -helix (around 1650 cm⁻¹) and β -turn (around 1663 and 1690 cm⁻¹). After assigning the bands using nine-point second-derivative analysis, the FTIR spectra were deconvoluted and fitted with OPUS software to quantify the individual peaks (Figures 7 and 8). The derivative spectrum of each untreated (or not dried) protein was overlaid on top of the corresponding dried protein. The assignment of each band to the secondary structural features after deconvolution is provided in Table 2. The peaks between

Table 2. Peak Assignments for Secondary Structure of Protein in D₂O of Deconvoluted Spectra in Amide I Region

component	wavenumber (cm ⁻¹)
β -sheet (low frequency)	1620–1640
random coil	1641–1647
α -helix	1648–1660
β -turns (low frequency)	1661–1673
β -sheet (high frequency)	1674–1680
β -turns (high frequency)	1681–1699

1600 and 1619 cm⁻¹ are known to be generated from aromatic side chains and are not considered during the quantification of secondary structure.^{16,31} The changes in the secondary structural features due to drying are provided in Table 3.

Table 3. Percentage Breakdown of Different Fractions of Secondary Structures in Native and Dried Whey Proteins

protein	treatment	secondary structures (%)			
		α -helix	β -sheet	β -turns	random coil
α -lac	native	35.00	39.50	20.00	5.50
	65 °C (dried)	32.50	41.50	18.50	7.50
	80 °C (dried)	29.50	46.00	15.00	9.50
β -lg	native	25.00	47.00	17.00	11.00
	65 °C (dried)	22.00	54.50	12.00	11.50
	80 °C (dried)	21.50	54.50	11.00	13.00
BSA	native	53.50	20.50	26.00	0.00
	65 °C (dried)	59.00	17.00	24.00	0.00
	80 °C (dried)	62.00	22.50	12.50	3.00

Thirteen bands were required to produce best fitting to α -lac and β -lg's IR spectra (Figure 7). On the other hand, BSA produced only five major bands in both native and dried states in the amides I region (Figure 8). Although the band numbers are similar in both native and dried proteins, they showed differences in magnitude and the location of the bands. Through the band fitting and quantification, it was found that the secondary structures of α -lac and β -lg are dominated by β structure, whereas the secondary structure of BSA is dominated by helix structure (Table 3). The observed composition of secondary structural features of BSA, α -lac, and β -lg is in

agreement with earlier studies.^{17,27,32} It has been reported that α -lac contains 41.0% β structure and 33.0% helix structure and that β -lg contains 50.0% β structure and 10.0% helix structure.²⁷ Similarly, BSA contains 24.0% β -sheet and 57.0% helix in its structure.^{17,32} Our observations suggest that the secondary structural properties of BSA, α -lac, and β -lg were affected by the convective drying quite differently. The drying process increased the β -sheet and random coil contents in β -lg by 7.5 and 2.0%, respectively. At the same time, the α -helix and β -turn contents decreased by 3.5 and 6.0%, respectively. In the case of α -lac, the drying stress decreased the α -helix content by 5.5% and the β -turn content by 5.0%. These decreased secondary structural contents were compensated by increases in β -sheet by 6.5% and random coil by 4.0%. The β -sheet, helix, and coil contents of BSA were found to increase (up to 2.0, 8.5, and 3.0%, respectively), whereas the β -turn content decreased (up to 13.5%).

In conclusion, the kinetics of major whey proteins revealed that at the end of 600 s of convective drying 13.3 and 19.4% α -lac was found to denature at 65 and 80 °C, respectively, whereas up to 31.0% of β -lg was denatured. No significant ($p > 0.05$) amount of BSA was found to be lost by denaturation under these drying conditions. The secondary structural properties of all the studied proteins were found to be significantly ($p < 0.05$) affected and altered by the drying stresses. In the case of α -lac and β -lg, the β -sheet and random coil contents were found to increase, which were compensated by the decrease in α -helix and β -turn. On the other hand, β -sheet, helix, and coil contents were found to increase in the case of BSA, whereas the β -turn content decreased. A highly wrinkled skin was formed on the surface of BSA, whereas a hollow fragile skin was formed on the surface of α -lac. The whey protein β -lg droplet lost its spherical shape initially but developed a firm outer surface skin afterward. The correlations among denaturation kinetics, drying kinetics, and particle morphology during drying at droplet level reported in this study will be important in producing structurally intact and functionally superior milk protein powders through spray-drying. The fundamental information on the denaturation kinetics of bovine serum albumin, α -lactalbumin, and β -lactoglobulin presented in this study will broaden the application of these proteins as nutritional and functional ingredients, especially in food and pharmaceutical applications.

AUTHOR INFORMATION

Corresponding Author

*E-mail: benu.adhikari@rmit.edu.au; Phone: +61 3 9925 9940; Fax: +61 3 992 53747.

Funding

M.A.H. thanks the Australian government for providing him with an Endeavour Postgraduate Scholarship.

Notes

The authors declare no competing financial interest.

ACKNOWLEDGMENTS

We thank Bruce Armstrong, Technical officer, Federation University Australia, for technical help during experiments.

REFERENCES

- (1) Oldfield, D. J.; Taylor, M. W.; Singh, H. Effect of preheating and other process parameters on whey proteins reactions during skim milk powder manufacture. *Int. Dairy J.* 2005, 15, 501–511.

- (2) Anandaramakrishnan, C.; Rielly, C. D.; Stapley, A. G. F. Effects of process variables on the denaturation of whey proteins during spray drying. *Drying Technol.* **2007**, *25*, 799–807.
- (3) Parris, N.; Baginski, M. A. A rapid method for the determination of whey protein denaturation. *J. Dairy Sci.* **1991**, *74*, 58–64.
- (4) Wehbi, Z.; Perez, M.; Sanchez, L.; Pocovi, C.; Barbana, C.; Calvo, M. Effect of heat treatment on denaturation of bovine α -lactalbumin: determination of kinetic and thermodynamic parameters. *J. Agric. Food Chem.* **2005**, *53*, 9730–9736.
- (5) Takeda, K.; Wada, A.; Yamamoto, K.; Moriyama, Y.; Aoki, K. Conformational changes of bovine serum albumin by heat treatment. *J. Protein Chem.* **1989**, *8*, 653–659.
- (6) Hosseini-nia, T.; Ismail, A. A.; Kubow, S. Pressure-induced conformational changes of β -lactoglobulin by variable-pressure Fourier transform infrared spectroscopy. *J. Agric. Food Chem.* **1999**, *47*, 4537–4542.
- (7) Lin, J.; Gentry, J. W. Spray drying drop morphology: experimental study. *Aerosol Sci. Technol.* **2003**, *37*, 15–32.
- (8) Adhikari, B.; Howes, T.; Bhandari, B. R.; Troung, V. Effect of addition of maltodextrin on drying kinetics and stickiness of sugar and acid-rich foods during convective drying: experiments and modelling. *J. Food Eng.* **2004**, *62*, 53–68.
- (9) Walton, D. E. The morphology of spray dried particles a qualitative view. *Drying Technol.* **2000**, *18*, 1943–86.
- (10) Ranz, W. E.; Marshall, W. R. Evaporation from drops. *Chem. Eng. Process.* **1952**, *48*, 141–146.
- (11) Sano, Y.; Keey, R. B. The drying of a spherical particle containing colloidal material into a hollow sphere. *Chem. Eng. Sci.* **1982**, *37*, 881–889.
- (12) Lin, S. X. Q.; Chen, X. D. Improving the glass-filament method for accurate measurement of drying kinetics of liquid droplets. *Chem. Eng. Res. Design* **2002**, *80*, 401–410.
- (13) Mezhericher, M.; Levy, A.; Borde, I. Theoretical models of single droplet drying kinetics: a review. *Drying Technol.* **2010**, *28*, 278–293.
- (14) Lin, S. X. Q.; Chen, X. D. A model for drying of an aqueous lactose droplet using the reaction engineering approach. *Drying Technol.* **2006**, *24*, 1329–1334.
- (15) Ferreira, I. M. P. L. V. O.; Caçote, H. Detection and quantification of bovine, ovine and caprine milk percentages in protected denomination of origin cheeses by reversed-phase high-performance liquid chromatography of β -lactoglobulins. *J. Chromatogr., A* **2003**, *1015*, 111–118.
- (16) Ngarize, S.; Herman, H.; Adams, A.; Howell, N. Comparison of changes in the secondary structure of unheated, heated, and high-pressure-treated β -lactoglobulin and ovalbumin proteins using Fourier transform Raman spectroscopy and self-deconvolution. *J. Agric. Food Chem.* **2004**, *52*, 6470–6477.
- (17) Fu, F.; Deoliveira, D. B.; Trumble, W. R.; Sarkar, H. K.; Singh, B. R. Secondary structure estimation of proteins using the amide III region of Fourier transform infrared spectroscopy: application to analyze calcium binding-induced structural changes in calsequestrin. *Appl. Spectrosc.* **1994**, *48*, 1432–1441.
- (18) van de Weert, M.; Haris, P. I.; Hennink, W. E.; Crommelin, D. J. A. Fourier transform infrared spectrometric analysis of protein conformation: effect of sampling method and stress factors. *Anal. Biochem.* **2001**, *297*, 160–169.
- (19) Kong, J.; Yu, S. Fourier transform infrared spectroscopic analysis of protein secondary structures. *Acta Biochem. Biophys. Sin.* **2007**, *39*, 549–559.
- (20) Huson, M. G.; Strounina, E. V.; Kealley, C. S.; Rout, M. K.; Church, J. S.; Appelqvist, I. A. M.; Gidley, M. J.; Gilbert, E. P. Effects of thermal denaturation on the solid-state structure and molecular mobility of glycinin. *Biomacromolecules* **2011**, *12*, 2092–2102.
- (21) Yang, W.; Griffiths, P. R.; Byler, D. M.; Susi, H. Protein conformation by infrared spectroscopy: resolution enhancement by Fourier self-deconvolution. *Appl. Spectrosc.* **1985**, *39*, 282–287.
- (22) Adhikari, B.; Howes, T.; Bhandari, B. R. Use of solute fixed coordinate system and method of lines for prediction of drying kinetics and surface stickiness of single droplet during convective drying. *Chem. Eng. Process.* **2007**, *46*, 405–419.
- (23) Haque, M. A.; Putranto, A.; Aldred, P.; Chen, J.; Adhikari, B. Drying and denaturation kinetics of whey protein isolate (WPI) during convective air drying process. *Drying Technol.* **2013**, *31*, 1532–1544.
- (24) Anandaramakrishnan, C.; Rielly, C. D.; Stapley, A. G. F. Loss of solubility of α -lactalbumin and β -lactoglobulin during the spray drying of whey proteins. *LWT—Food Sci. Technol.* **2008**, *41*, 270–277.
- (25) Haque, M. A.; Aldred, P.; Chen, J.; Barrow, C. J.; Adhikari, B. Comparative study of denaturation of whey protein isolate (WPI) in convective air drying and isothermal heat treatment processes. *Food Chem.* **2013**, *141*, 702–711.
- (26) Yazdanpanah, N.; Langrish, T. A. G. Comparative study of deteriorative changes in the ageing of milk powder. *J. Food Eng.* **2013**, *114*, 14–21.
- (27) Byler, D. M.; Susi, H. Examination of the secondary structure of proteins by deconvolved FTIR spectra. *Biopolymers* **1986**, *25*, 469–487.
- (28) Boye, J. I.; Alli, I.; Ismail, A. A.; Gibbs, B. F.; Konish, Y. Factors affecting molecular characteristics of whey protein gelation. *Int. Dairy J.* **1995**, *5*, 337–353.
- (29) Ng-Kwai-Hang, K. F. *Milk Proteins Heterogeneity, Fractionation, and Isolation*; McGill Univ. Mont. QC; Elsevier: Canada, 2011; pp 751–764.
- (30) Adhikari, B.; Howes, T.; Bhandari, B. R.; Troung, V. Surface stickiness of drops of carbohydrate and organic acid solutions during convective drying: experiments and modeling. *Drying Technol.* **2003**, *21*, 839–873.
- (31) Susi, H.; Byler, D. M. Fourier deconvolution of the amide I Raman band of proteins as related to conformation. *Appl. Spectrosc.* **1988**, *42*, 819–826.
- (32) Grdadolnik, J. Saturation effects in FTIR spectroscopy: intensity of amide I and amide II bands in protein spectra. *Acta Chim. Slov.* **2003**, *50*, 777–788.